

Modeling of Pavement Behavior in Tropical Hot and Dry Conditions: Numerical Approach and Comparison on Road Section

Sidpouita Mathilde Koudougou · David Yemboini Kader Toguyeni

Laboratory of Physics and Chemistry of the Environment (LPCE)-University JKZ-UFR / SEA-03 BP 7021Ouagadougou, Burkina Faso.

ABSTRACT

The purpose of this article is to propose a two-dimensional (2D) model in finite element of distribution of the temperatures and deformations in extreme weather conditions of Burkina Faso (heat wave, heavy showers) using the software COMSOL Multiphysics. This model takes into account the hourly weather conditions (solar radiation, air temperature, air humidity, dew temperature, wind speed) as well as the temperature dependence of the mechanical parameters (elastic modulus, poisson ratio) of the asphalt pavement materials. The obtained results show that it's possible to identify, for periods of the day, the existence of nonlinear and permanent deformations at the level of the superficial layers of the pavement. The meteorological factor proved to be more than decisive in the choice of bitumen used for the realization of asphalt pavement in tropical zones.

© 2020 JMSSE · Indian Thermal Spray Society · Science IN. All rights reserved

ARTICLE HISTORY

Received 19-11-2019
Revised 12-02-2020
Accepted 20-02-2020
Published 21-04-2020

KEYWORDS

Thermal Modelling
Simulation
Pavement
Sky Temperature
Urban Drainage

Introduction

The study of heat transfers in the pavement is a means used by researchers to solve various problems with the same objective; that of predicting the pavement temperature profile. Work has been carried out in the direction of temperature forecasting in an attempt to answer questions about the influence of temperature on the functional and structural performance of pavements in different weather conditions; to understand the effects of freezing and thawing [1], humidity [2], the impact of temperature variations on deflection and response to mechanical stresses [3], the non-uniformity of damage to the pavement [4].

Two types of approaches are used to predict pavement temperatures. These are the analytical method and the statistical method. The analytical approach was the first method used to determine pavement surface temperature [5]. It is based on theories heat and mass transfer and the thermal properties of asphalt pavement. It consists in solving the heat equation with the energy balance on the pavement surface.

The statistical approach requires the acquisition of many experimental pavement measurements and meteorological data. It is based on the processing and statistical analysis of collected pavement temperature data for different weather conditions in order to establish correlations with relevant parameters.

The modeling of hygrothermal transfers in the pavement is located in the literature as an extended study of heat transfer modeling. Excluding heat transfers in pavements depends on weather conditions, including precipitation and snow. The researchers who were interested in the study of heat transfers in the pavement do not take into account precipitation in meteorological conditions [4, 6-7]. Taking precipitation and/or snow into account would open the prediction of pavement temperature to all weather conditions. The modeling of hygrothermal transfers makes it possible to offer pavement design engineers calculation

tools that increase the accuracy of temperature prediction for a more rational pavement design [8].

Two approaches are used to evaluate the action of water on pavement temperature. Some researchers hypothesize that the flow of water film from precipitation is instantaneous and that there is no accumulation of rain on the pavement surface [9].

Burkina Faso is served by a network of 2654,482 km pavements in full expansion to meet the societal and economic challenges. The periodic maintenance of this network increases because their deterioration occupies a significant part of the budget allocated to the ministry in charge of infrastructure particularly since increasing of pavement in asphalt concrete realization.

Climate change conditions increase vulnerability to deterioration of these road infrastructures. At periods of warm weather for example there is an expansion of the pavement. Observations, models, but also pale hydrological studies identify the potential of climate change as having a direct impact on the realization of road infrastructures [10]. In Burkina Faso, users, observations and media talk about the amplification of pavement degradation. In addition, feedback from pavement design engineers indicates that climate change is not taken into account in the construction of road in Burkina Faso.

As far as we are informed, the question of pavement behavior in the face of thermal has not yet been scientifically studied in Burkina Faso. Pavements are built using old methods of pavement that take climate into account from the notion of equivalent temperature [11]. However, they currently do not make it possible to reduce pavement deterioration problems related to meteorological fluctuations, so equivalent temperature is not correct.

Deformation and fatigue behavior of bituminous mixtures that vary with temperature, loading and pavement degradation levels fluctuate during the year with temperature cycles [12]. It is obvious that the prediction of

pavement behavior in order to avoid early degradation appears to be a necessity.

The objective of this article is to study with COMSOL Multiphysics 5.2a modeling tool how to predict the distribution of temperatures and deformations of some asphalt concrete pavement in the extreme weather conditions of Burkina Faso that consist in heat waves and heavy showers.

Experimental

Materials

The chosen pavement for this study to predict the damages on its surface is a National Road 4(NR4). It is located east of Ouagadougou City. It was constructed in 2018. In this study, we are focused on the section kilometric point (KP), KP2+675 and KP2+850. From a geotechnical point of view, NR4 is a draining pavement made of four layers: Surface or wearing course, Base course in asphalt concretes and Sub-base course, Soil subgrade.

Asphalt concrete layers

Asphalt concretes are impermeable materials used in the wearing course (AC) and the base course (BC) of the pavement. They are composed of a mixture of crushed granites and pure bitumen. Granites originate from Yimdi's career on the West side of Ouagadougou City. The granular skeleton of the wearing course (AC) consists of particle size classes 6/10, 4/6, 0/4 and that of the base course (BC) are 0/4, 4/6, 6/10, 10/14 size classes.

Bitumen

Pure bitumen 35/50 is the binder used for the formulation of asphalt concretes mixtures. These features are arranged in the Table 1.

Table 1: Bitumen identification

Bitumen	ρ (kg/m ³)	Penetrability	TBA (°C)
35/50	1025	38.66	54.75

Sub-base course

The Sub-base course is obtained by litho stabilization named Lithostab [13]. The litho stabilization is a technique that consists in improving the bearing capacity of the lateritic gravel used at the base of pavements by adding a quantity of crushed granite determined accordingly. Lithostab used in this work is a mixture of 30% crushed granite from the Yimdi's career and gravel laterite clay from Banogo 12° 18' 14" North whose geotechnical properties are shown in the Table 2.

Soil subgrade

A lateritic clayey gravelly (LCG) is a residual soil of tropical weathering, consisting of a mixture of particles generally between 2 and 20 mm in size (pisolites, concretions or nodules more or less hard and or quartz) and lateritic clay of color mostly reddish or ocher (sometimes gray, further north of the country). The gravelly clayey lateritic used have geotechnical properties shown in the Table 2.

Table 2: Geotechnical characteristic of Lithostab and LCG

Mixes Identification	Size distribution (%)			Plasticity index (I_p)	Modified Proctor		I_{CBR} à 95% OPM
	0.08mm	2mm	10mm		w_{OPM} (%)	ρ_d (g/cm ³)	
Lithostab	18	31	70	13	7.3	2.240	68
LCG	24.5	34	87.5	14	9.3	2.15	49

Numerical Model

The pavement is often considered in the literature as a homogeneous semi-infinite, isotropic, linear viscoelastic solid medium at low temperatures and impermeable to water [14]. It is not supposed to produce energy translated by zero internal heat flux (zero geothermal gradient) and submit meteorological conditions [15] (Fig 1).

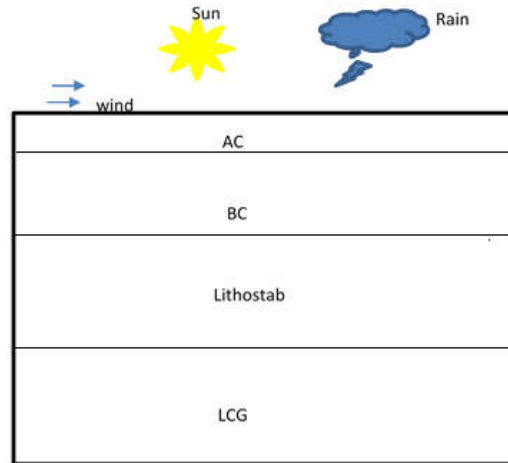


Figure 1: model description

Governing equations

Transient conduction

The equation governing heat transfer in the different layers of the pavement is given by:

$$\Delta T = \frac{1}{D} \frac{\partial T}{\partial t} \tag{1}$$

Where T (°C) is the temperature; $D = \frac{k}{\rho C_p}$ ($m^2 s^{-1}$) the thermal diffusivity of each layer k is the thermal conductivity ($W m^{-1} K^{-1}$), ρ is the density $Kg m^{-3}$ and C_p is the specific heat ($J Kg^{-1} K^{-1}$).

Thermal Energy balance

The pavement is subject to weather conditions and traffic. In these conditions, the net energy (W/m^2) available on its surface which is then transferred by conduction to the different layers is given by the following relation [16] :

$$\varphi_{net} = \varphi_a + \varphi_r + \varphi_{cond} \pm \varphi_{conv} \tag{2}$$

φ_a : energy absorbed from direct solar radiation
 φ_r : energy emitted from the pavement towards the sky
 φ_{cond} : energy transferred to or from the pavement by conduction
 φ_a and φ_r are always positive for all the structure such as pavement exposed to radiation.

φ_{conv} , the convection energy is transferred from the pavement to the surrounding air if the former has a higher temperature than the latter. During a rainy episode, the energy balance on the pavement surface takes the following form [8]:

$$\varphi_{net} = \varphi_a + \varphi_r + \varphi_{cond} \pm \varphi_{conv} - \varphi_{rain} + \varphi_e \quad (3)$$

φ_{rain} : energy induced by the fall the shower
 φ_e : latent energy

Radiation energy

There are two components in the radiation energy at the surface of the pavement: Sun irradiates short wavelength (SWL) energy onto the pavement surface. One part of his energy is absorbed by the pavement surface causing a rising of the pavement temperature. This energy is given by :

$$\varphi_a = (1 - \alpha)R_g \quad (4)$$

Where $R_g(W/m^2)$ is a solar radiation; For our purpose, α , the albedo of the pavement surface is taken equal to 0.18 [15].

Pavement irradiates the long wavelength (LWL) energy towards the sky according to the Stefan-Boltzmann law:

$$\varphi_r = \sigma \epsilon (T_{sky}^4 - T_s^4) \quad (5)$$

Where $\sigma = 5.669 \times 10^{-8} (Wm^2K^{-4})$ is the Stefan-Boltzmann constant; ϵ emissivity of the pavement surface is taken equal 0.92 [14]; $T_{sky} (K)$ sky temperature; $T_s (K)$ surface temperature.

Conduction energy

Conduction energy $\varphi_{cond}(W/m^2)$ from the pavement surface down can be approximately calculated as [17] :

$$\varphi_{cond} = -k \frac{T_z - T_s}{z} \quad (6)$$

Where $T_z (K)$ is temperature of the pavement at depth $z (m)$.

Convection energy

The pavement surface undergoes the phenomena of natural convection.

Natural convection is energy transfer between air and the pavement surface $\varphi_{conv}(W/m^2)$. It's given by Newton's Law:

$$\varphi_{conv} = h_c(T_s - T_{air}) \quad (7)$$

Where h_c is convective exchange coefficient; $T_{air} (K)$ the air temperature

The Wind speed, $V_{wind} (m/s)$ of Ouagadougou is generally lower than 5 (m/s) at 30m from the ground[18], so we chose empirical expression of convective exchange coefficient Given by[14, 16].

$$h_c = 5.8 + 4.1 \times V_{wind} \quad (8)$$

Energy induced by the fall of the rain

The fall of the rain generates sensitive energy $\varphi_{rain}(W/m^2)$ given by the following relation [8].

$$\varphi_{rain} = 3,6 \times 10^{-6} \times i \times \rho_w \times C_{pw}(T_{rain} - T_s) \quad (9)$$

Where $i(mm/h)$ the rain intensity; $\rho_w(Kg/m^3)$ density of rain water; $C_{pw}(\frac{J}{Kg^{\circ}C})$; $T_{rain}(K)$ temperature of rain.

Latent Energy

The water coming from the rain that is available on the surface of the pavement is subjected to the phenomenon of evaporation described by the relation below [8-9].

$$\varphi_e = h_{fg} \times \dot{m}_w'' C_{pw}(w_{air} - w_s) \quad (10)$$

Where $h_{fg}(Kg/(sm^2))$ is the latent heat of vaporization and is computed from the relationship [19]; $\dot{m}_w''(Kg)$ the mass transfer of evaporating water; $w_{air}, w_s (\%)$ are humidity ratio of the ambient air and humidity ratio of saturated air at the pavement surface obtained using correlations given by [20].

Thermal strains

The strains induced by thermal stresses have a given mechanical response by [21].

$$\epsilon_T = \epsilon_m + \epsilon_{th} = \alpha_{th} \Delta T \quad (11)$$

Where ϵ_T is total strain, ϵ_m is mechanical strain equal to zero, ϵ_{th} the thermal strain, α_{th} thermal expansion ratio.

Finite element modeling with Comsol Multiphysics 5.2

Principle of FEM transient heat transfer modelling

Practical heat transfer problems are described by the partial differential equations with boundary conditions. The numerical methods allow obtaining the approximate values of unknowns at discrete points called nodes. One of them, is a finite element method (FEM) developed and applied to solve numerous heat transfer problems [22]. FEM method requires division of the problem domain into many sub domains for which the heat transfer problem is analyzed. Each sub domain is called the finite element; thus, the name of this method is the finite element method [23].

Pavement finite element modeling with Comsol Mutiphysics 5.2 Software

The numerical model is based on a finite element method using the COMSOL Multiphysics 5.2 software. The inputs data's are dimensions of the pavement layers (thickness, length or width), properties of layers materials (density, conductivity, thermal expansion coefficient, specific heat capacity, stiffness modulus), hourly time evolutions of climatic parameters (solar radiation, Temperature and humidity of air, convective exchange coefficient and sky clarity index, dew point temperature in sky temperature calculation).

The outputs are the profiles of temperature fields along the depth, the profiles of temperature and flow rate, stresses which associate of chosen position of the pavement during a period at 06 :00 a.m to 06 : 00 p.m.

Results and Discussion

The model presented was simulated in extreme climatic conditions. That means the historical days of 06 April 2018

for the dry season and some rainy days corresponding to frequencies of rain appearance of 2 years, 5 years, 10 years for the rainy season. It corresponded to the following values of intensity: 12.5mm/h, 12.7mm/h and 15mm/h.

Initial condition

The initial condition chosen was obtained by theoretical calculation. Indeed, the general solution of the heat equation (1) can take the following real form:

$$T(z, t) = \bar{T} + A \sin(\omega t - \varphi(z)) \quad [24] \quad (12)$$

where \bar{T} is the average hourly temperature ; $A = A_0 e^{-kz}$ where A_0 is the amplitude of daily temperature fluctuations and z the depth ; $\varphi = kz$ is the phase ; $k = \sqrt{\frac{\pi}{D\tau}}$; k : thermal conductivity ; $D = \frac{k}{\rho C_p}$ thermal diffusivity ; C_p : specific heat capacity ; ρ density ; τ : the period of daily temperature fluctuations

In the following, it is assumed that the initial temperature in each of the layers of the pavement is equal to the average temperature between the temperature at the upper face of the layer and that of the lower face.

The initial solution form at the surface of AC layer is given by: $T(z_{up}; AC = 0, t = 0) = \bar{T} + A \sin(0 - \varphi(0)) = \bar{T}$. Thus, initial solution at z depth of AC layer is given by :

$$T(z_{AC}, t = 0) = \bar{T} + A \sin(0 - \varphi(0)) = \bar{T} + A \sin(0 - \varphi(z)) = \bar{T} + A \sin(-\varphi(z)) = \bar{T} - A_0 e^{-k_{AC}z_{AC}} \sin(k_{AC}z_{AC}) \quad (13)$$

We chose the average temperature between the upper side and the upper side average temperature of the AC layer:

$$T_{AC} = \frac{[T(z_{dow,AC}, t = 0) + T(z_{up,AC} = 0, t = 0)]}{2}$$

$$\text{or } T_{AC} = T(z_{up,AC}, t = 0) - \frac{A_0 e^{-k_{AC}z_{AC}} \sin(k_{AC}z_{AC})}{2} \quad (14)$$

The Initial solution on the surface of the BC or at the interface between AC and BC is :

$$T(z_{up,BC}, t = 0) = T_{AC} - A_0 e^{-k_{AC}z_{AC}} \sin(k_{AC}z_{AC}) \quad (15)$$

The same process is repeated for subsequent layers. \bar{T} chosen is the average temperature measured on the surface of the pavement from 1 to 6 April 2018 at 6 : 00 a.m. Assuming that the amplitude of the pavement fluctuations during the day equals to that of the air during the same day, A_0 is the difference between the maximum and minimum of air temperature from 1 to 6 April 2018 between 6:00 a.m and 6:00 p.m. The results are arranged in the Table 3.

Table 3: Initial temperatures of the pavement layers

\bar{T} at 6h	A_0	T_{AC}	T_{BC}	T_{LGC}	$T_{LITHOSTAB}$
23.8°C	19.5°C	21.1°C	15.7°C	15.6°C	15.6°C

Sky Temperature

Many expressions are used to evaluate sky temperature. In this studied, we chose the following expression because it

presents explicitly the optical effect of aerosols through clearness index of the sky [25].

$$T_{sky} = 94.12 \ln(P_v) - 13 I_c + 0.314 T_{air} \quad (16)$$

where I_c : clearness index of the sky; P_v partial vapor pressure

Meteorological and geometric parameters

The meteorological data used for the simulations come from the General Directorate of Meteorology of Burkina Faso. These are hourly values from 6:00 a.m to 6:00 p.m of solar radiation, air temperature, dew temperature, air humidity, wind speed, water depth.

The numerical model is two-dimensional 2D that takes into account the thickness and length to simulate when the pavement is dry. Width and longitudinal slope of the pavement is taken in the 2D numerical model when the pavement is wet by a shower.

Thermo-physical parameters

The thermal conductivities of the four layers have been measured (Table 4). The others thermo-physical parameters such as thermal expansion coefficient [21, 26] and specific heat capacity were taken from the literature [27-29].

Table 4: Thermo-physical properties of the pavement layers

Mixes Identification	k (W /mK)	C_p (J/kg /°C)	ρ (kg /m³)	α_{th} (°C ⁻¹)
AC	1.702	900 Ref. [28, 29]	2260	2.5×10^{-5} Ref. [21, 26]
BC	1.584	900 Ref. [28, 29]	2300	2.5×10^{-5} Ref. [21, 26]
Lithostab	0.77	900 Ref. [27]	2240	
LCG	0.67	600 Ref. [27]	2120	

Geotechnical parameters

All the geotechnical parameters of the pavement are stored in the Table 5, that is to say stiffness modulus and Poisson ratio. It should be noted that the stiffness modulus of the asphalt concrete are chosen depending on the temperature T (°C) at a fixed frequency of 10Hz.

Table 5: Stiffness modulus E and poisson ratio ν of AC and BC layers

	E (Pa)	ν
AC	$-1018.1T^3 + 181094T^2 - 10^7T + 2 \times 10^8$	$0.15 + 0.35/(1 + \exp(3.1849 - 0.04233 \times T(^{\circ}F)))$ Ref. [6,30]
BC	$-1181.1T^3 + 210294T^2 - 10^7T + 2 \times 10^8$	$0.15 + 0.35/(1 + \exp(3.1849 - 0.04233 \times T(^{\circ}F)))$ Ref. [31,32]
Lithostab	$3.4 \times 10^8 Pa$	0.4 Ref. [33]
LCG	$1.47 \times 10^8 Pa$	0.4 Ref. [33]

The modules of the Sub-base course and Soil sub grade (Table 5) are obtained by applying the empirical relationships [9] :

$$E_{Lithostab} = 50 \times I_{CBR} \quad (17)$$

$$E_{LCG} = 30 \times I_{CBR} \quad (18)$$

Validation of the model and influence of the temperature of the sky

When comparing the temperature measurements made on the surface of the pavement by infrared thermometer with simulations obtained using Aubinet, Bliss and Berdhal models [24, 33, 34] the sky temperature expressions, showed the same overall appearance (Fig 2.).

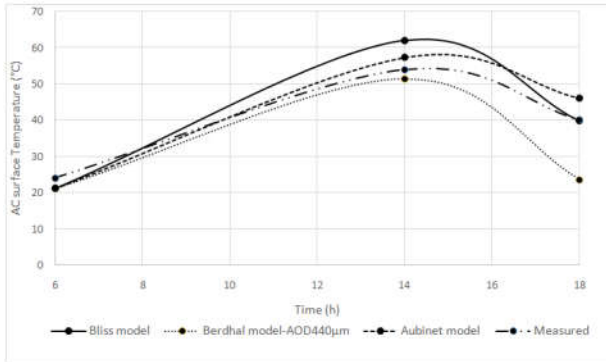


Figure 2: AC surface Temperature simulated with three models evaluating Sky Temperature

The model with the expression proposed by Bliss, commonly used in the literature corresponds best because it presents a quadratic error between simulations and measurements: 1.7°C with Bliss expression, 2.2°C with Aubinet expression and 4.1°C with Berdhal expression. We selected the model using the expression proposed by Aubinet because it presents a quadratic error superior to that proposed by Berdhal while explicitly taking into account the influence of the aerosols through the clearness index of the sky.

Sensitivity Analysis

Sensitivity analysis quantifies the overall significance of the model's input parameters on their ranges of variation. The method of analysis of Moris used in the case of dynamic modeling consists of identifying beforehand the influential parameters and then classifying them according to their influence [35].

$$\text{We define the sensitivity } S = \frac{\Delta D / D}{\Delta P / P} \quad (19)$$

Where P is the parameter; D (m) the total displacement of the pavement; ΔD (m), ΔP the variation of the displacement and that of the parameter associated with the displacement [36].

Sensitivity to physically-thermal and geotechnical properties of the pavement

The results of the sensitivity analysis are stored in the table 6. The lowest order corresponds to the most sensitive parameter. Sensitivity can be ordered in descending order: $S_p > S_{c_p} > S_k > S_e > S_\alpha$ and $S_{L_x} = S_\epsilon = 0$. Thus, simulation results are independent with the length of the pavement.

Sensitivity to initial temperature of the pavement layers

In Burkina Faso, the climate analysis stipulates a minimum average temperature of 15.3°C and a maximum average temperature of 42.4°C at Dori (North) over the observation years of 1983-2012 (Fig 3.).

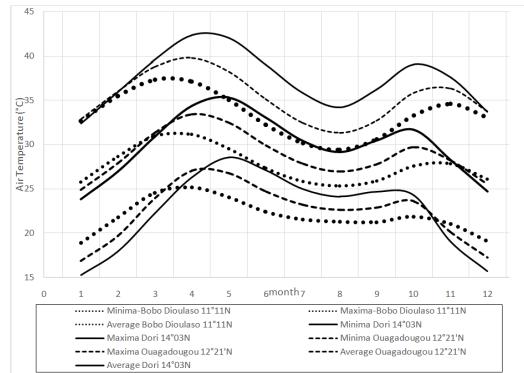


Figure 3: Air Temperature evolution (1983-2012) in Burkina Faso

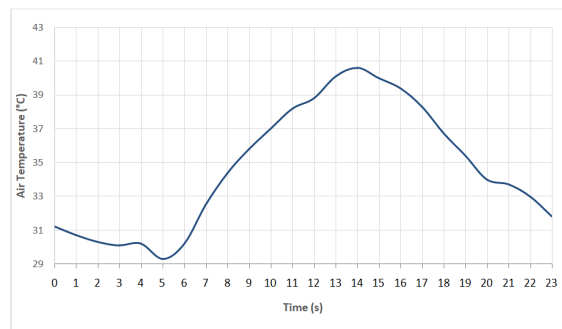


Figure 4: Air Temperature evolution for a Typical Day of April (1992-2006)

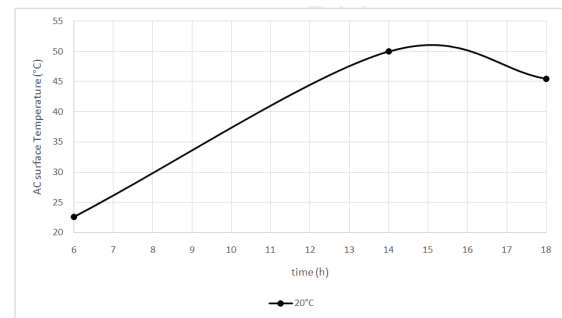


Figure 5: sensitivity to Initial Temperature for different values of \bar{T}

Table 6: Sensitivity analysis

P	S	S order
k (W m/K)	1.14E-01	3
depth (m)	1.06E-01	4
Length (m)	0.00E+00	6
ϵ	0.00E+00	6
α	5.54E-02	5
AOD	0.00E+00	6
C_p (J/kg/°C)	2.68E-01	2
ρ (kg/m³)	2.86E-01	1

When we focus on a typical day of the month of April in the city of Ouagadougou [37], the minimal temperature is 11.3°C against a maximum temperature above 40°C (Fig 4.) with an average air temperature of 29.3°C at 6:00 a.m. So, two sensitivity analyzes to the initial temperature parameters \bar{T} and A_0 were performed.

The first analysis was carried out in the temperature range of the month of April and the second in the extreme range of the climate of Burkina Faso. In the temperature range of April the sensitivity analysis of the model indicates that a

slight variation does not affect the results of the simulation (Fig 5.).

Indeed, the sensitivity analysis (Table 6) carried out for the initial temperature parameter \bar{T} at 20, 22, 26°C resulted in an almost zero standard deviation.

Effect of temperature on mechanical behavior: dry pavement

Evolution of the field of the temperature

The graph of the field of the pavement temperature (Fig6.) indicates a damping of the surface temperature towards the bottom of the pavement confirmed by many authors [3, 6,38].

The temperature at the surface of the AC, part exposed to meteorological conditions is higher than that of the BC, then the Lithostab and the LCG (Fig 7, 8).

Meteorological conditions induce a deformation of the pavement layers quantified (Fig 9-12).

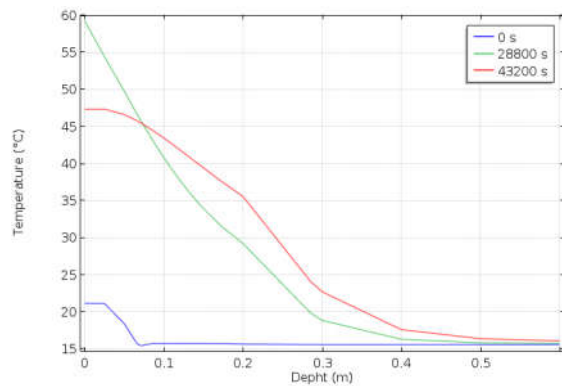


Figure 6: Spatial Temperature evolution of pavement with depth pavement depth (m)

Effect of temperature on mechanical behavior: dry pavement

The time curve analysis of the temperatures indicates that from approximately 9h 15min, the surface temperature of the pavement is higher than the softening point temperature of the bitumen (54.75°C) until 17h 45min. The simulated maximum temperature at the surface of the pavement at 2:00p.m is about 62.6°C. At6:00 a.m (t = 0s simulation time), the temperature between AC and BC is reduced, about 4°C. At 6:00 p.m (t = 43200s), the difference is therefore 18°C (Fig 7.). There would be a warming of the pavement structure from 6:00 a.m. to 06:00 p.m. The pavement would accumulate energy during the day. The temperature of a layer changes as the temperature of the air. A phase shift or lag in time between the temperature of the air and the surface of the pavement is observable on the (Fig 8.)This phase difference confirms the contribution with its accumulation and the restitution of energy of the pavement. The pavement is therefore an infrastructure with high inertia. The stiffness modulus of the mixes varies proportionally with the temperature of the layer considered and the expansion ratio inversely proportional to the temperature [39].

In our study, we chose polynomial functions to represent the temperature dependency of the stiffness modulus for a reference frequency of 10Hz. Mechanical deformations evolves with temperature over time. They are remarkable at the level of the upper layers of the pavement (AC and BC) and negligible in the lower layers (Lithostab, LCG) (Fig 9-12).

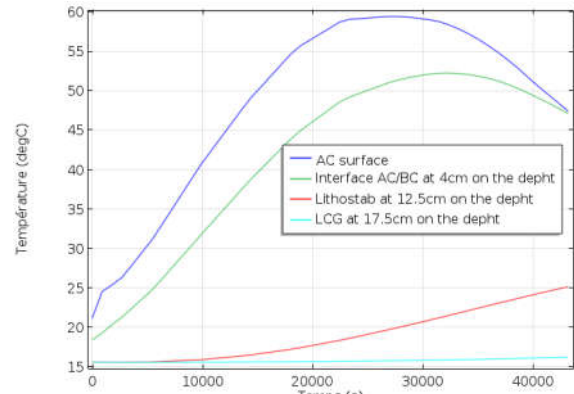


Figure 7: Temperature evolution of pavement layers

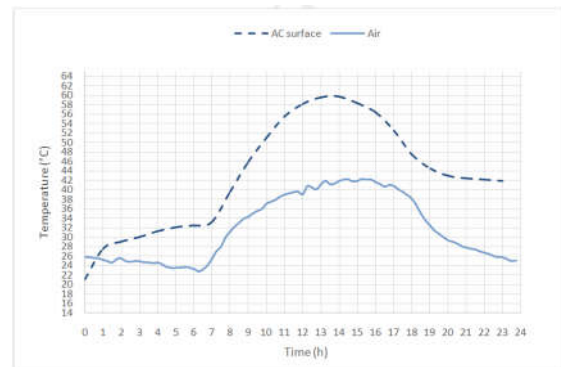


Figure 8: Phase shift between Air Temperature and AC surface Temperature

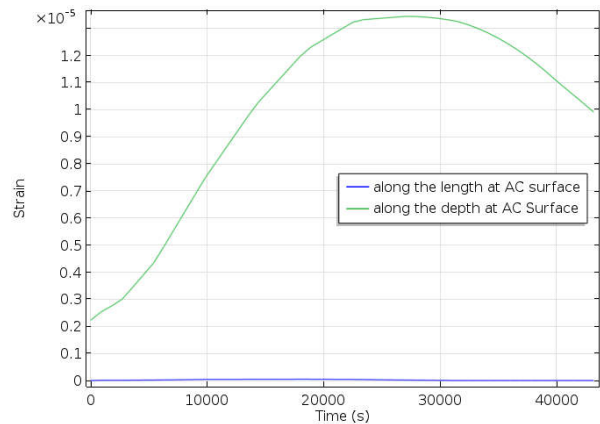


Figure 9: Strain along the length and the depth of AC

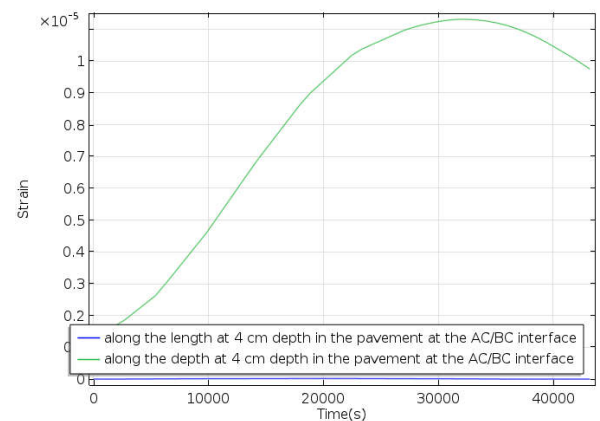


Figure 10: Strain along the length and the depth of BC

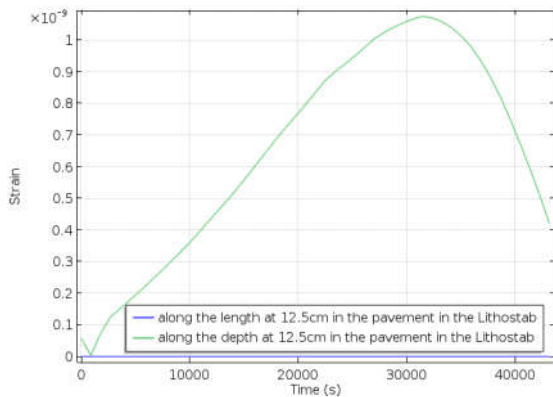


Figure 11: Strain along the length and the depth of Lithostab

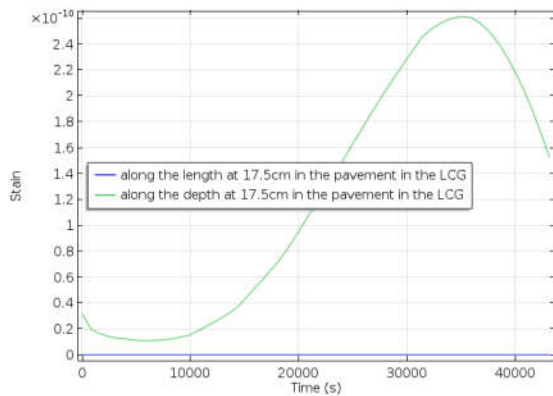


Figure 12: Strain along the length and the depth of LCG

Table 7: Maximum strain along pavement length (X) and depth (Y)

Layers	Strain-max X	Strain-max Y	LOG (Strain-max X)	LOG (Strain-max Y)
AC	4.94E-08	1.35E-05	-7.31	-4.87
BC	2.21E-08	1.14E-05	-7.66	-4.94
Lithostab	0	1.19E-09		
LCG	6.80E-12	5.46E-10		

According to Di Benedetto's [40] classification for the obtained deformation ranges, we can deduce that the behavior of the surface layers of the pavement responds to the linear viscoelastic deformation regime according to the depth along the length of the pavement (Table 7). Longitudinal deformations and the deformations in the direction of the depth are admissible [41]. Under traffic conditions, if the deformations with depth become 10 times greater, the surface layers will have a non-linear response and exceed the permissible values. These permanent deformations, which will be the consequence of an accumulation of non-linear deformations, can be assimilated to ruts. Consequently, the 35/50 bitumen will not be adapted in the hot climate conditions in Burkina Faso.

Effect of rain on thermal behavior: wet pavement

Evolution of the field of the temperature

The graph of the field of temperature show for a rain intensity of 15.2 mm/ over a period of 3 hours, the order of evolution of the temperatures in the different layers of the pavement is respected because of the duration of the rain. The work of Kertesz et al. [41] has shown that over

rainy periods of about 8 minutes (small showers), the temperature on the surface of the AC is below that of the BC. We think that is because latent heat exchanges are more important than sensible heat exchanges when the rainfall is longer.

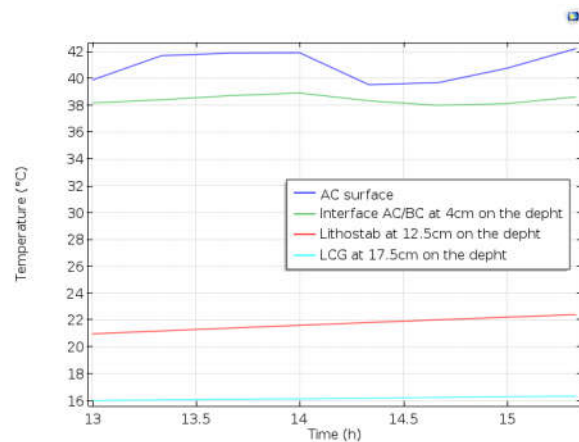


Figure 13: Pavement layers temperature evolution during the shower

Evolution of temperature with showers intensities

If the temperature difference between AC and BC is constant during the first hour of rain, it varies in subsequent hours due to the greater sensitivity of the AC to rain. The analysis of the above graphs of the surface temperatures of the pavement indicates that the rainy episode leads to a decrease of the temperatures thus a cooling of the surface of the pavement. The maximum rain intensity corresponds to the minimum temperature on the surface of the pavement (Fig 14.) having taken care to locate the rainy episode at the time of the hottest day between 2:00 p.m and 5:00 p.m, the observation is that the temperatures are always lower than the softening point of the bitumen.

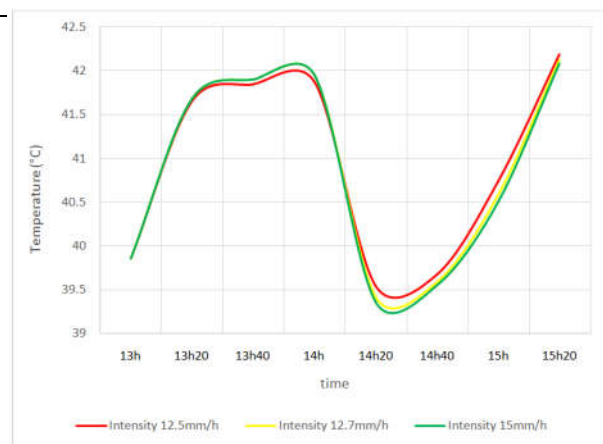


Figure 14: Temperature of pavement for different shower intensities

Conclusions

This work has focused on frequency of the standard frequency of 10Hz, the effect of tropical canicular and wet weather conditions on a pavement made with bitumen 35/50. The model was built by adding thermal dependence laws of materials most susceptible to temperature (AC and BC). It also explicitly takes into account the hourly weather

conditions from 6:00 a.m to 6:00 p.m GMT, determining the radiative energy emitted by the pavement through Aubinet relationship and determined the temperature profiles in the pavement. In warm meteorological conditions, the simulations carried out showed that over a period of 8h30, between 9:00 a.m and 6:00 p.m, the surface temperature of the pavement exceeded the temperature of the softening point of the bitumen that equal 54.75°C. This period of the day unfortunately corresponds to periods of heavy road traffic increasing the appearance of blisters visible on the surface of the pavement. Under rainy conditions, the pavement temperature remains below the softening point of the bitumen due to the wet weather conditions and the cooling induced by the shower.

Acknowledgment

We would like to express our gratitude to: The Cooperation Service of the French Embassy in Burkina Faso for funding this project; the National Laboratory of Building and Public Works of Burkina Faso, especially, Professor Anne PANTET and Doctor Tariq OUAHBI of the Laboratoire Ondes et Milieux Complexes (France) for advices. Mister Ali SANA and his team including Mister Justin SAWADOGO and Mister Serge TIEMTORE for their geotechnical help of the Laboratoire du Bâtiment et des Travaux Publics (Burkina Faso); the General Direction of Meteorology, particularly Mister Kouka OUEDRAOGO who made available the weather data. Doctor Ali KONFE for is numerical help.

References

- Dempsey, B. J., A heat transfer model for evaluating frost action and temperature related effects in multi layered pavement systems, Highway Research Record No 342. National Research Council, Washington, D.C., 1970, 39 – 56.
- Ali, H., and Lopez, A, Statistical analysis of temperature and moisture effects on pavement structural properties based on seasonal monitoring data, Transportation Research Record 1540, Transportation Research Board, Washington, D.C., 1996, 48–55.
- Southgate H.F., Deen R.C., Temperature Distribution within Asphalt Pavements and Its Relationship to Pavement Deflection. Lexington: Kentucky Department of Highways, Research Report, 1968.
- Marshall, C., MeierR., Welch M., Seasonal Temperature Effects on Flexible Pavements in Tennessee, Transportation Research Board of the National Academies, Washington, D.C., 2001, 89–96.
- Barber, E.S., Calculation of Maximum Pavement Temperatures From Weather Reports, Highway Research Board Bulletin, 1957, 168 : 1-8.
- Thompson M.R., B.J. Dempsey H. Hill J. Vogel, Characterizing Temperature Effects for Pavement Analysis and Design. In : Transportation Research Record: Journal of the Transportation Research Board, No. 1121, Transportation Research Board of the National Academies, Washington, D.C., 1987, 14–22.
- Hermansson, A., A Simulation Model for the Calculation of Pavement Temperatures, Including the Maximum Temperature, Transportation Research Record, 1699, 134 - 141, 2000.
- Chiasson A.D, Yavuzturk C., K. Ksaibati, Linearized Approach for Predicting Thermal Stresses in Asphalt Pavements due to Environmental Conditions, Mater. Civil. Eng., 2008, 118–127.
- Yavuzturk, C., Ksaibati, K., Chiasson, A. D., Assessment of Temperature Fluctuations in Asphalt Pavements Due to Thermal Environmental Conditions Using a Two Dimensional, Transient Finite-Difference Approach, J. Mater. in Civil Eng., 17(4), 465–475, 2005.
- Daniel J.S, ASCE M., Jacobs J.M, Douglas E., B. Rajib, Mallick, K. Hayhoe, Effects on Pavement and Geotechnical Infrastructure, Climatic Effects on Pavement and Geotechnical Infrastructure, 2017, 1-9.
- Centre expérimental de Recherches et d'Etudes du bâtiment et des travaux publics, Guide pratique de dimensionnement des chaussées pour les pays tropicaux , 1984, 106-117.
- Himeno K., Watanabe T., Maruyama T., Temperature distributions in asphalt pavements, in Proceedings of the 3rd Paving in Cold Areas, Canada/Japan Science and Technology Agreement Mini Workshop, Ottawa. W.H. Highter, D.J. Wall, Thermal properties of some asphaltic concrete mixes, Transp. Res. Rec, 1984.
- Lompo P., les matériaux utilisés en construction routière en Haute-Volta, un matériau non traditionnel, le LITHOSTAB, IRF IVe CONFERENCE ROUTIERE AFRICAINE 20-25 Janvier 1980 Nairobi, Kenya, 29-40.
- Asfour S., Récupération d'énergie dans les chaussées pour leur maintien hors gel, PhD thesis, Université Blaise Pascal Clermont, 2017, 115 262.
- Hall M.R., Dehdezi P.K., Dawson A.R., Grenfell J., and Isola R., Influence of the thermophysical properties of pavement materials on the evolution of temperature depth profiles in different climatic regions. Journal of Materials in Civil Engineering, 2012, 24 , 32–47.
- Sheeba J. B, Rohini, A. K. Structural and Thermal Analysis of Asphalt Solar Collector Using Finite Element Method, Journal of Energy, 2014.
- Solaimanian M., Kennedy T.W., Predicting Maximum Pavement Surface Temperature Using Maximum Air Temperature and Hourly Solar Radiation, Transportation Research Record, Journal of the Transportation Research Board, 1417, 1993, 1–11.
- Landry M, Ouedraogo Y, Gagnon Y, Ouedraogo A, Atlas éolien du Burkina Faso, 2011, 18.
- Irvine, T. F., Jr., and Liley, P. E., Steam and gas tables with computer equations, Academic, 1984.
- ASHRAE, ASHRAE handbook, fundamentals, American Society of Heating, Refrigerating and Air, Conditioning Engineers, Inc., Atlanta, 2001.
- Di Benedetto H., Neifar, M., Coefficients de dilatation et de contraction thermiques d'un enrobé bitumineux avec et sans chargement mécanique, Mechanical Tests for Bituminous Materials, Proceeding of the 5th International RILEM Symposium, 1997, pp 421-428.
- Kavianipour A, Beck V. Int J, Heat Mass Transfert, 1977, 20(3), 259–67.
- Lewis. R.W., Nithiarasu P., Seetaramu K N, Fundamentals of the Finite Element method for Heat and Fluid Flow, 2004.
- Carslaw. M.S, Jaeger J.C , 1954, Conduction of heat in solids, Oxford Science publications.
- Aubinet, M., Longwave sky radiation parameterizations ", Solar Energy, 53, 1994, 147- 154.
- Olard F., Comportement thermomécanique des enrobés bitumineux à basses températures. Relations entre les propriétés du liant et de l'enrobé, PhD thesis, Institut national des sciences appliquées de Lyon, 2003, 138.
- Ensley, E. K., Petersen, J. C., and Robertson, R.E., 1984, Thermochemica Acta, 77, 95- 107.
- Highter WH, Wall DJ. Thermal properties of some asphaltic concrete mixes. Transp Res Rec 1984, 968 : 38–45.
- Islam M.R., Tarefder R.A., Determining thermal properties of asphalt concrete using field data and laboratory testing, Constr. Build. Mater., 2014, 67(2), 38-40.
- Bari J., Witczak M., Development of a new revised version of the predictive model for hot mix asphalt mixtures, Journal of the Association of Asphalt Paving Technologists, 75 : 381–423, 2006.
- Maher, A., Bennert, T. A. , Evaluation of Poisson's ratio for use in the mechanistic empirical pavement design guide (MEPDG), 2008.

32. Mirza M. W., Development of Relationships to Predict Poisson's Ratio for Paving Materials, University of Maryland, College Park, MD, Inter-team Technical Report for NCHRP 1-37A, 1999.
33. Bliss, R. W., Atmospheric radiation near the surface of the ground, Sol. Energy, 1961.
34. Berdahl, P., Martin M., Emissivity of clear skies, Solar Energy 32(5), 1984, 663-667.
35. Morris, M.D., Factorial Sampling Plans for Preliminary Computational Experiments, Technometrics, 1991, 33(2), 161-174.
36. Matmat, M., Thèse de Doctorat, Pour une approche complète de l'évaluation de fiabilité dans les micro-systèmes, Université de Toulouse, 2009, 158, 49.
36. Ouedraogo E., Elaboration d'une année météorologique type de la ville de Ouagadougou pour l'étude des performances énergétiques des bâtiments, Revue des Energies renouvelables, 15(1), 2012, 77-90.
37. Ulmeta L., Petita C., Mokhtari A.M., Temperature modelling in pavements: the effect of long- and short-wave radiation, International Journal of Pavement Engineering, 2014.
38. Wang H., S.Wu, M. Chen, Y. Zhang, Numerical simulation on the thermal response of heat-conducting asphalt pavements, IOP PUBLISHING, 2010.
39. Di Benedetto H., Nouvelle approche du comportement des enrobés bitumineux: résultats expérimentaux et formulation rhéologique, Mechanical Tests for Bituminous Mixes, Characterization, Design and Quality Control, Proceedings of the Fourth Rilem Symposium, 1990.
40. LCPC-SETRA, Conception et dimensionnement des structures de chaussée, Guide Technique, Paris 1994.
41. Kertesz, R., Sansalone, J. Hydrologic Transport of Thermal Energy from Pavement. Journal of Environmental Engineering, 2014, 140(8), 4014028.

